Available online at www.sciencedirect.com
ScienceDirect
Applied Surface Science 253 (2007) 3444–3449
applied surface science
www.elsevier.com/locate/apsusc

Functionalization of lamellar molybdenum disulphide nanocomposite with gold nanoparticles

V. Lavayen [a,b,*], C. O'Dwyer [a], M.A. Santa Ana [b], N. Mirabal [b], E. Benavente [c], G. Cárdenas [d], G. González [b], C.M. Sotomayor Torres [a]

[a] Tyndall National Institute, University College Cork, Lee Maltings, Prospect Row, Cork, Ireland
[b] Department of Chemistry, Faculty of Sciences, Universidad de Chile, P.O. Box 653, Santiago, Chile
[c] Department of Chemistry, Universidad Tecnológica Metropolitana, P.O. Box 9845, Santiago, Chile
[d] Department of Polymers, Faculty of Chemistry Science, Universidad de Concepción, P.O. Box 160-C, Concepción, Chile

Received 29 May 2006; accepted 12 July 2006
Available online 22 August 2006

Abstract

This work explores the functionalization of an organic–inorganic MoS_2 lamellar compound, prepared by a chemical liquid deposition method (CLD), that has an interlamellar distance of ~5.2 nm, using clusters of gold nanoparticles. The gold nanoparticles have a mean diameter of 1.2 nm, a stability of ~85 days, and a zeta potential measured to be $\zeta = -6.8$ mV (solid). The nanoparticles are localized in the hydrophilic zones, defined by the presence of amine groups of the surfactant between the lamella of MoS_2. SEM, TEM, EDAX and electron diffraction provide conclusive evidence of the interlamellar insertion of the gold nanoparticles in the MoS_2.

PACS: 61.66.−f; 68.35.−p; 68.37.−d; 72.80.−r; 73.25.+i

Keywords: Colloid; Nanoparticles; Molybdenum; Functionalization

1. Introduction

The study of the chalcogenide compounds has gained considerable interest in recent times [1] and, in particular, the investigation of novel kinds of approaches in the synthesis of organic–inorganic lamellar compounds [2] has been achieved using polymers [3], metals [4], organometallic compounds [5], and surfactants [6]. It has also been reported that co-intercalation techniques employing lamellar compounds [7] resulted in the formation of nano-hybrids [8] and their potential applications were also explored.

Over the last decade, the number of reports in the literature in the area of nano-science has increased very rapidly [9]. A pertinent example is that of nanoparticles and indeed their formation is one of the most interesting areas in materials science due to their unusual properties, which can be considerably different to those of their corresponding macro-crystalline bulk material [10]. These unique chemical and electronic properties have potential applications in the fields of non-linear optics, luminescence, electronics, optoelectronics and others [10,11]. Examples of typical routes to functionalize not only certain nanocomposites, but also nanotubes [12], include acid-based wet-chemical oxidation, esterification, diimide activation, electrochemical modification, or hydrophobic adsorption of aromatic derivatives [13–17]. These techniques, however, typically entail multiple steps involving reflux reactions with strong acids combined with ultrasonication, which are aggressive treatments.

The most relevant approach for the preparation of stable metallic colloids using the chemical liquid deposition method (CLD) in organic solvents is based on the clustering of metal atoms at low temperature [10]. This method has been used with volatile solvents to prepare several colloidal suspensions of transition metals of the first and second rows [10,11]. The colloidal particles thus obtained are free of interferences and impurities, in contrast to those obtained from aqueous solutions.

* Corresponding author. Tel.: +353 21 490 4391; fax: +353 21 490 4467.
E-mail address: vlavayen@tyndall.ie (V. Lavayen).

0169-4332/$ – see front matter
doi:10.1016/j.apsusc.2006.07.039

In this paper we present results of an investigation towards of the functionalization of the $Li_{0.1}MoS_2(HDA)_2$ lamellar compounds with gold nanoparticles prepared with the chemical liquid deposition method (CLD). Such a functionalization approach enables the maturation of a simple and more readily scalable derivatization method.

2. Experimental

Molybdenum disulfide powder (particle size <2 mm) (Aldrich); hexadecylamine (HDA) 92%, *n*-butyl lithium and *n*-hexane solution (Merck) were used as received. Water was twice distilled and carefully degassed.

2.1. Synthesis of lamellar MoS_2 compounds

The method employed for the synthesis of molybdenum disulfide nanocomposite was essentially the same as that described in [1]. Lithium-intercalated MoS_2, previously prepared by direct intercalation of lithium using *n*-BuLi (Li_xMoS_2, $x > 1$), is exfoliated by a 24 h moisture treatment. The product is then prepared into an aqueous suspension. Amine–MoS_2 nanocomposites are prepared by addition of an aqueous solution of amine to the suspension of exfoliated MoS_2, followed by stirring of the reaction mixture at 323 K for 48 h.

2.2. Preparation of Au–acetone colloid

The metal–atom reactor (3L) used was described elsewhere [10]. As a typical example of preparation, 70 mg Au metal was placed into the alumina–tungsten crucible. Dry acetone was placed in a ligand inlet tube and freeze–pump–thaw degassed in several cycles. The reactor was pumped down to 4–5 mmHg, while the crucible was warmed to red heat. The vessel around the crucible was cooled with liquid nitrogen and Au and acetone (100 ml) were deposited for a period of 1 h using a current intensity of 40 A. The matrix was allowed to warm under vacuum for 1 h; upon meltdown to room temperature, a purple colloid was obtained. Subsequently the addition of nitrogen up to 1 atm, the colloid was allowed to warm for another 0.5 h to room temperature. The solution was siphoned into a flask cooled in atmospheric nitrogen from the acetone inlet. The typical molarity of the metal-containing solution is $\sim 4 \times 10^{-3}$ mol dm^{-3}.

2.3. Incorporation of gold nanoparticles (Au-NPs) in $Li_{0.1}MoS_2(HDA)_2$

20 mg of the $Li_{0.1}MoS_2(HDA)_2$ was agitated for 4 h with a colloidal solution of gold (Au-nanoparticles) in acetone at room temperature. In this case, the solvent was added in excess to ensure the solvation of the metal atoms.

2.4. Characterization of samples

The morphology of the lamellar nanocomposite was examined by scanning electron microscopy (SEM) using a Philips XL-30 equipped with an energy-dispersive spectroscopy (EDS) detector. Transmission electron microscopy was obtained on a JEOL JEM 1200 EXII operating at 100 kV.

2.5. Selection area electron diffraction (SAED)

The electron diffraction of the nanoparticles was obtained using the JEOL microscope internally calibrated with a gold standard (Merck, 99.99% purity; 120 kV, $K = 3.848$ cm Å). The diffraction patterns were obtained using a limiting field aperture 20 mm. In this way, the diffraction from the grid is avoided and the observed area is minimized. The chemical composition of the samples was determined by elemental chemical analysis (SISONS model EA-1108).

3. Results and discussion

Fig. 1 shows an SEM micrograph of the lamellar $Li_{0.1}MoS_2(HDA)_2$. The bulk laminarity of the nanocomposite is clearly observed. Previous X-ray diffraction studies by our group show that the nanocomposite exhibits a high degree of crystallinity evidenced by the observation of defined {0 0 l} peaks [1]. From these {0 0 l} planes, the interlamellar distance measured to be 5.17 nm. The compound exhibits a 4.55 nm (Δc) difference in the interlamellar separation with respect to the pristine compound (0.615 nm) [1]. This distance measurement is in good agreement with our previous report [18] on lamellar MoS_2. Fig. 2 shows a TEM micrograph of the laminar nanocomposite and associated electron diffraction pattern. Elemental analysis of the compound $Li_{0.1}MoS_2(HDA)_2$ yields the following, C: 56.8, N: 3.8, S: 9.0, H: 10.6%, with a theoretical percentage of N: 4.4, C: 60.5, S: 10.6, H: 9.6%.

Observation of the organic–inorganic nanocomposite using electron microscopy not only showed the presence of the lamellar structure but electron diffraction data also showed the presence of a ring indicative of the {1 0 0} plane (Fig. 2) with a reinforcement at the corners of a hexagon (locally intense diffraction spots) that arise from reflections of the {1 0 3} plane [19], outlined in Table 1. Thus, these observations confirm the presence of a hexagonal phase in the nanocomposite with a

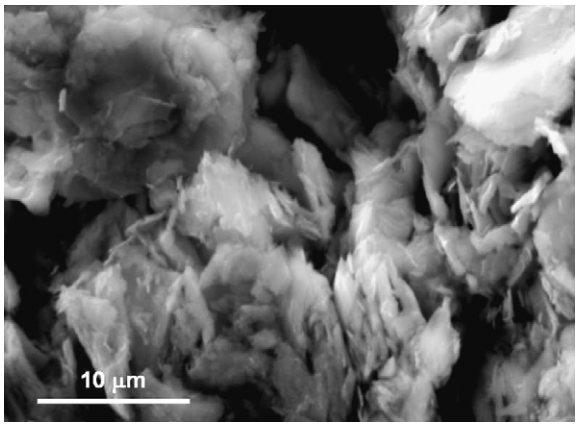

Fig. 1. SEM image of the $Li_{0.1}MoS_2(HDA)_2$ lamellar product prior to funtionalization with gold nanoparticles.

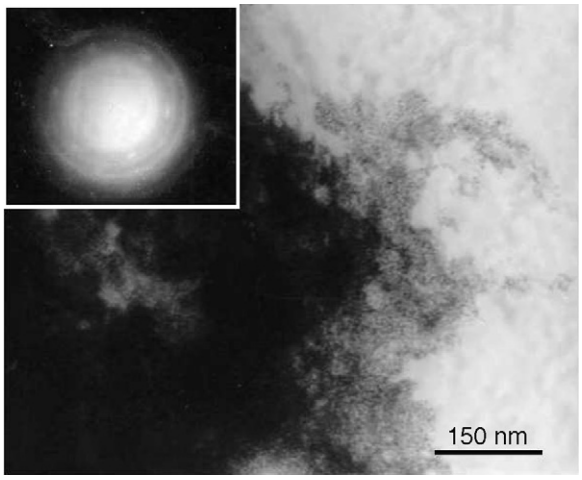

Fig. 2. TEM image of the $Li_{0.1}MoS_2(HDA)_2$ compound prior to functionalization. (Inset) Electron diffraction pattern of the same lamellar nanocomposite.

calculated lamellar distance of the {0 0 2} plane measured to be 0.30 nm, in good agreement with our XRD observations [18].

The average particle size was determined using TEM, shown in Fig. 3. By estimating the density, ρ, of gold nanoparticles as a function of diameter (shown in Fig. 3B), an average size for the gold nanoparticles throughout the dispersion is estimated at ~1.2 nm. The measurements of the particle population diameters are randomly chosen; an average of 100 particles were counted in each micrograph allowing for a relatively accurate estimated of the average size. The histograms were obtained using the Origin 6 program [20] which gives information on the particle size distribution.

Fig. 3A and B shows dark- and bright-field TEM micrographs, respectively, of the functionalized lamellar compound showing the presence of interlamellar gold nanoparticles. A high degree of crystallinity was found using electron diffraction (ED) and the polycrystalline nature of the gold nanoparticles (Au-NPs) within the lamellar product is evidenced by the characteristic ring patterns. Fig. 3C shows the electron diffraction pattern obtained and five characteristic diffraction spots corresponding to the {2 0 0}, {2 2 0}, {3 1 1}, {2 0 0} and {4 0 0} planes of the fcc crystalline lattice were observed; the assignation to crystal planes is outlined in Table 2. The electron diffraction measurements of the Au-NPs show that they have an anisotropic crystalline structure [21,22]. Fig. 3D shows a histogram of measurements of individual gold nanoparticles made by TEM; the gold nanoparticles exhibit a mean diameter of 1.2 nm, as outlined above. We found that the

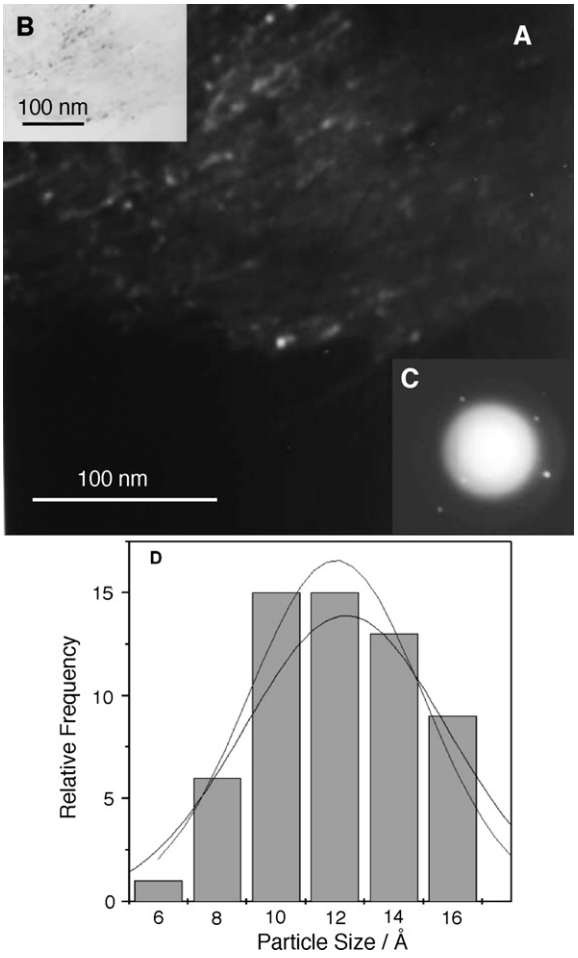

Fig. 3. Dark-field TEM image of the gold nanoparticles (Au-NPs) in acetone ([Au]: 4×10^{-3} mol dm^{-3}) (A). Bright-field TEM micrograph of randomly dispersed gold nanoparticles (B) and corresponding electron diffraction pattern (C). Histogram of Au-NPs size distribution. Gaussian fits are overlaid for comparison giving an average value of 1.2 nm for the nanoparticle diameter (D).

particle sizes in this colloid are shorter than those of typical individual colloids showing lower kinetic stability. Furthermore, the Au-nanoparticles/acetone metallic colloid exhibits a zeta potential of $\zeta = -6.8$ mV (solid), showing a high stability for the measurement of electrophoretic mobility, a result comparable with previous reports [10].

One particular difficulty in microscopically quantifying the effectiveness of $Li_{0.1}MoS_2(HDA)_2$ functionalization by bright-field TEM is that the presence of the gold nanoparticles is not clearly visible, as apparent from Fig. 4A. By employing dark-field imaging of the {0 0 2} reflection of gold (Fig. 4B), we

Table 1
Electron diffraction indexation of the observed planes of the $Li_{0.1}MoS_2(HDA)_2$ compound

Phase	$d_{h\,k\,l}$ (nm)	Diffraction plane
MoS_2	0.28[a]	{0 0 2}
MoS_2	0.22	{1 0 0}
MoS_2	0.19	{1 0 3}

[a] Calculated from the electron diffraction spot.

Table 2
Electron diffraction indexation of the gold nanoparticles

Phase	$d_{h\,k\,l}$ (nm)	Diffraction plane	Au standard $d_{h\,k\,l}$ (nm)
Au	0.16	{2 0 0}	0.16
Au	0.15	{2 2 0}	0.14
Au	0.12	{3 1 1}	0.11
Au	0.11	{2 2 2}	0.10
Au	0.10	{4 0 0}	0.08

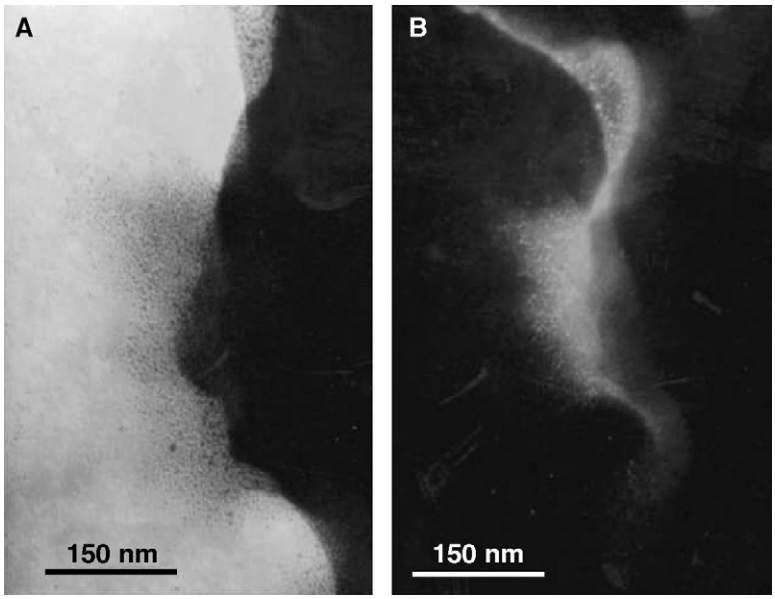

Fig. 4. TEM Image of the $Li_{0.1}MoS_2(HDA)_2$ compound after the functionalization with gold nanoparticles in bright-field mode (A); and dark-field mode (B).

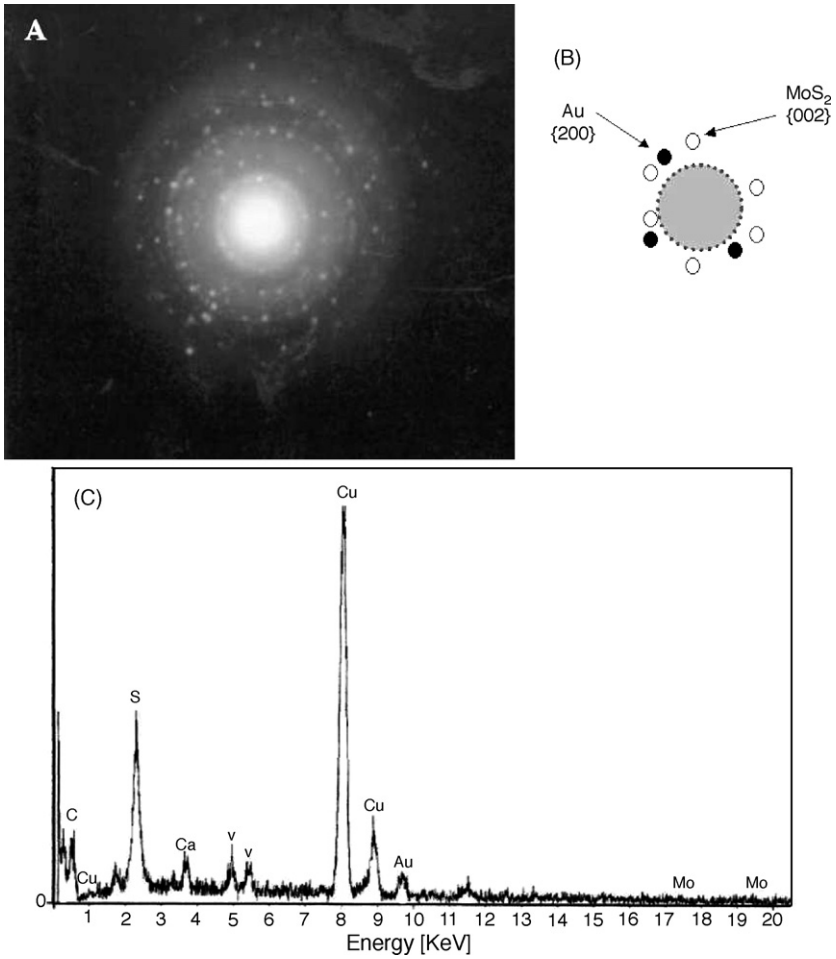

Fig. 5. (A) Electron diffraction pattern of the $Li_{0.1}MoS_2(HDA)_2$ compound after the functionalization with gold nanoparticles and (B) indexation of the contributions from MoS_2 and Au{1 1 1}. (C) Energy dispersion spectroscopy analysis of the same compound.

observed the presence of brilliant points (metallic particles) at the borders of the layers. These regions correspond to the area where gold nanoparticles are present. For instance, using electron diffraction we observed the presence of two phases in the system: one containing the gold nanoparticles and the other the MoS_2 phase. The electron diffraction pattern is reproduced in Fig. 5A and analytical details for the diffraction spot assignation are outlined in Table 3. A schematic representation of the diffraction spots corresponding to both the Au and MoS_2 phase contributions is shown in Fig. 5B. This information conclusively verifies the presence of gold nanoparticles in the system (on the surface or resident in the interlamellar space of the host), but due to the high gold affinity of the thiols, it is difficult to ascertain the location of the nanoparticles with high precision.

To determine the exact location of the gold nanoparticles, we analyzed some areas using EDS, shown in Fig. 5C. The intense Cu signal is that of the Cu grid. In spite of the presence of the intense copper peak, it was possible to detect the presence of a small fraction of gold, indicating that the majority of the gold nanoparticles are located inside the lamellar spacings. The presence of the vanadium and calcium contributions arises from the trace impurities of the as-received molybdenum disulfide (99% pure).

Careful examination of the electron diffraction spots in Fig. 5A shows evidence of an hexagonal phase corresponding to the {0 0 0 2} basal plane of MoS_2 in a similar position as those from the {2 0 0} plane of the polycrystalline fcc gold nanoparticles (Table 3). Thus, the location of the gold nanoparticles is between the hexagonally ordered MoS_2 lamella in the vicinity of the hydrophillic zone of the surfactant.

A possible scheme to explain the residence of the gold nanoparticles inside the lamellar compound after functionalization is outlined in Fig. 6. In this scheme, we propose that the residual negative charge (ζ-potential) on the nanoparticle cluster by the presence of oxygen groups (keto, hydroxo) of the surfactant in the nanoparticle/acetone colloid, corroborated by our previous infrared analysis [10], facilitates their preferred nucleation and attachment to the functionalized zones of the nanocomposite by the surfactant. The negatively charged Au-nanoparticles are localized in the hydrophilic zones, defined by the presence of amine groups of the surfactant. Because we have not used any molecular coupling agents to cap the nanoparticles themselves, we deduce the presence of hydrophilic zones due to the presence of the surfactant to be the locations where the gold nanoparticles are attached to the MoS_2 lamella.

Table 3
Electron diffraction indexation of the functionalized $Li_{0.1}MoS_2(HDA)_2$ compound with gold nanoparticles (Au-NPs)

Phase	$d_{h\,k\,l}$ (nm)	Diffraction plane	Au standard $d_{h\,k\,l}$ (nm)
Au	0.21	{1 1 1}[a]	0.23
Au	0.19	{2 0 0}	0.16
Au	0.12	{1 1 1}	0.14
Au	0.10	{3 1 1}	0.10
Au	0.08	{2 2 2}	0.09
MoS_2	0.14	{0 0 2}	–

[a] Calculated from the electron diffraction spot.

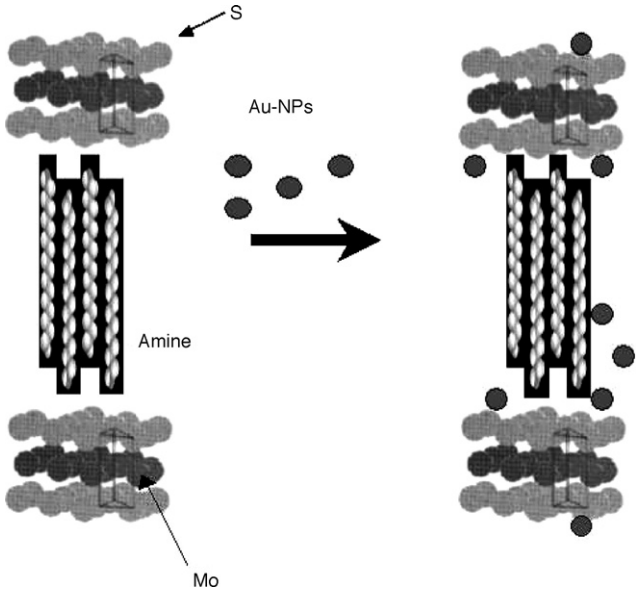

Fig. 6. Schematic representation of the functionalization of the $Li_{0.1}MoS_2(HDA)_2$ compound with gold nanoparticles and their position in the lamellar system. The MoS_2 is represented in the 1T conformation [1].

4. Conclusions

In this communication, we have successfully demonstrated the functionalization of lamellar molybdenum disulphide nanocomposite using gold particles prepared by the chemical liquid deposition method (CLD). We observed the presence of the gold nanoparticles mainly inside the MoS_2 lamella in the vicinity of the hydrophilic zone of the surfactant. The next stage will involve the improvement of the structural measurements using other complimentary techniques, focusing on the particle–surfactant interface with the purpose to explore their tribological properties.

Acknowledgements

The support of the FONDECYT (Grants 1050344, 1030102, 7050081), Science Foundation Ireland (SFI), PHOREMOST, the University de Chile, and the Universidad Tecnologica Metropolitana are gratefully acknowledged.

References

[1] E. Benavente, M.A. Santa Ana, F. Mendizábal, G. González, Coord. Chem. Rev. 224 (2002) 87.
[2] R. Bissessur, P.K.Y. Liu, Solid State Ionics 177 (2006) 191.
[3] G. Hwang, V. Petkov, K.K. Rangan, S. Shastri, M.G. Kanatzidis, J. Phys. Chem. B 106 (2002) 12453.
[4] V. Sánchez, E. Benavente, M.A. Santa Ana, G. González, Chem. Mater. 11 (1999) 2296.
[5] B.-Z. Lin, X.-K. Pei, J.-F. Zhang, G.-H. Han, Z. Li, P.-D. Liu, J.-H. Wu, J. Mater. Chem. 14 (2004) 2001.
[6] B.A. Vanchura, P. He, V. Antochshuk, M. Jaroniec, A. Ferryman, D. Barbash, J.E. Fulghum, S.D. Huang, J. Am. Chem. Soc. 124 (2002) 12090.
[7] J. Iranmahboob, H. Toghiani, D.O. Hill, Appl. Catal. A 247 (2003) 207.
[8] C.M. Julien, Mater. Sci. Eng. R 40 (2003) 47.
[9] M.H.A. Hassan, Science 309 (2005) 65.

[10] G. Cárdenas, J. Chil. Chem. Soc. 50 (2005) 603.
[11] R.A. Segura, J. Reyes-Gasga, G. Cárdenas, Colloid Polym. Sci. 282 (2004) 1206.
[12] M.S. Raghuveer, S. Agrawal, N. Bishop, G. Ramanath, Chem. Mater. 18 (2006) 1390.
[13] A. Rinzler, J. Liu, H. Dai, P. Nikolaev, C.B. Huffman, F. Rodriguez-Macias, P.J. Boul, A.H. Lu, D. Heymann, D.T. Colbert, R.S. Lee, J.E. Fischer, A.M. Rao, P.C. Eklund, R.E. Smalley, Appl. Phys. A 67 (1998) 29.
[14] S.H. Qin, D.Q. Oin, W.T. Ford, D.E. Resasco, J.E. Herrera, J. Am. Chem. Soc. 126 (2004) 170.
[15] S.S. Wong, E. Joselevich, A.T. Woolley, C.L. Cheung, C.M. Lieber, Nature 394 (1998) 52.
[16] K. Balasubramanian, R. Sordan, M. Burghard, K. Kern, Nano Lett. 4 (2004) 827.
[17] R.J. Chen, Y. Zhang, D. Wang, H. Dai, J. Am. Chem. Soc. 123 (2001) 3838.
[18] G. González, M.A. Santa Ana, E. Benavente, V. Sánchez, N. Mirabal, Mol. Cryst. Liq. Cryst. 374 (2002) 229.
[19] J. Moser, H. Liao, F. Levy, J. Phys. D: Appl. Phys. 23 (1990) 624.
[20] OriginLab Corporation, Northampton, MA 010060, USA.
[21] C.Y. Tsai, D.S. Lee, Y.H. Tsai, B. Chan, T.Y. Luh, P.J. Chen, P.H. Chen, Mater. Lett. 58 (2004) 2023.
[22] K. Page, T. Proffen, H. Terrones, M. Terrones, L. Lee, Y. Yang, S. Stemmer, R. Seshadri, A.K. Cheetham, Chem. Phys. Lett. 393 (2004) 385.